

Towards Solving QCD in Light-Cone Quantization –
On the Spectrum of the Transverse Zero Modes for SU(2).

Hans-Christian Pauli and Rolf Bayer

Max-Planck-Institut für Kernphysik

D-69029 Heidelberg

30 September 1995

Abstract

The formalism for a non-abelian pure gauge theory in (2+1) dimensions has recently been derived within Discretized Light-Cone Quantization, restricting to the lowest *transverse* momentum gluons. It is argued why this model can be a paradigm for full QCD. The physical vacuum becomes non-trivial even in light-cone quantization. The approach is brought here to tractable form by suppressing by hand both the dynamical gauge and the constraint zero mode, and by performing a Tamm-Dancoff type Fock-space truncation. Within that model the Hamiltonian is diagonalized numerically, yielding mass spectra and wavefunctions of the glue-ball states. We find that only color singlets have a stable and discrete bound state spectrum. The connection with confinement is discussed. The structure function of the gluons has a shape like $[x(1-x)]^{\frac{1}{3}}$. The existence of the continuum limit is verified by deriving a coupled set of integral equations.

1 Introduction and Motivation

Constructing even the lowest state that is the ‘vacuum’ of a Quantum Field Theory has been so notoriously difficult that the conventional Hamiltonian approach was given up altogether, long ago in the Fifties. It was overlooked that other forms, particularly Dirac’s ‘front form’ of Hamiltonian dynamics [1] might have less severe problems. In fact, concretely realizing the front form with periodic boundary conditions one might combine the aspects of a simple vacuum [2] with a careful treatment of the infrared degrees of freedom. The method referred to is Discretized Light-Cone Quantization (DLCQ) [3]. A review can be found in [4]. Potentially, the method is able to reconcile the simplistic but otherwise successful constituent quark picture of Feynman’s parton model [5] with the low-energy regime of Quantum Chromodynamics (QCD) as the fundamental theory of hadrons. But the conversion of this non-perturbative method into a reliable tool for hadronic physics is bestowed with many difficulties [6], one of them being the so-called ‘zero mode problem’.

Recently, (2+1) dimensional pure SU(2) gauge theory has been examined suppressing transverse gluon momentum excitations [7]. The dimensionally-reduced theory turns out to be SU(2) gauge theory in (1+1) dimensions coupled to adjoint scalar matter. A topological (gauge) mode appears coupled to true dynamical Fock modes of the transverse gluon fields. Moreover, a constrained zero mode appears which is defined by a linear but still very complicated equation, whose inversion is far from being trivial [8], structures that were foreseen by Franke et al. [9] in (3+1) dimensions. Such types of models, first discussed in DLCQ by [10, 11, 12, 13] but without zero modes and assuming only color singlet string states, enable insight into how to overcome the obstacles in the full theory.

Next to interesting vacuum structures [8], the dimensionally reduced model of QCD has a fascinating excitation spectrum whose structure is difficult to guess, see [7]. It is this latter point to which we address ourselves in the present work. We do that at the expense of rigor, keeping only the Fock space structure of the model to be presented below in detail. Despite the heavy truncations the present work has rather interesting aspects, which can serve as paradigms for what one expects in full QCD.

2 Formulation of the Model

The model [7] considered in the sequel is a (1+1) dimensional non-abelian gauge theory covariantly coupled to scalar adjoint matter whose Lagrangian density is given by

$$\mathcal{L} = \text{Tr} \left(-\frac{1}{2} \mathbf{F}^{\alpha\beta} \mathbf{F}_{\alpha\beta} + \mathbf{D}^\alpha \Phi \mathbf{D}_\alpha \Phi - \mu_0^2 \Phi \Phi \right). \quad (1)$$

The color electro-magnetic fields are the usual ones in matrix notation, *i.e.*

$$\mathbf{F}^{\alpha\beta} \equiv \partial^\alpha \mathbf{A}^\beta - \partial^\beta \mathbf{A}^\alpha + ig[\mathbf{A}^\alpha, \mathbf{A}^\beta] \equiv \partial^\alpha \mathbf{A}^\beta - \mathbf{D}^\beta \mathbf{A}^\alpha. \quad (2)$$

The covariant derivative \mathbf{D}_α is the carrier of ‘longitudinal gauge invariance’ which is not affected by adding a mass term. Fixing the gauge

$$\text{Tr}(\tau^\pm \mathbf{A}^+) = 0, \quad \partial_- \mathbf{A}^+ = 0, \quad \text{and} \quad \text{Tr} \langle \tau^3 \mathbf{A}^- \rangle_0 = 0, \quad (3)$$

completes the model. With the purpose of setting the notation we recall here in short the most important steps of Ref.[7].

For SU(2), the above τ^a are 2×2 matrices related to the Pauli spin matrices σ_i . They define a color helicity basis in terms of which all fields are expanded, *i.e.*

$$\tau^3 = \frac{1}{2} \sigma_z, \quad \tau^\pm \equiv \frac{1}{2\sqrt{2}} (\sigma_x \pm i\sigma_y), \quad \text{thus} \quad \Phi = \tau^3 \varphi_3 + \tau^+ \varphi_+ + \tau^- \varphi_-. \quad (4)$$

We shall be careful to have the Lorentz and color indices consistently raised and lowered, respectively, when we write down individual field components. Since the matrices are traceless and hermitean, one deals with nine real-valued operator functions, three for each field. Gauge fixing, *i.e.* $\mathbf{A}^+ = v\tau^3$, reduces the problem to six real-valued operator functions and one quantum mechanical operator $v \equiv v(x^+)$, which one keeps track of in the combination $z \equiv vgL/\pi$. Four out of these seven have a non-vanishing conjugate momentum, particularly the momenta canonically conjugate to v , φ_3 , φ_- , and φ_+ . Only these are therefore ‘independent fields’ subject to be quantized. The vector potential v (thus z) is quantized like a quantum mechanical variable [14] that is like $[z, p_z] = i$, with the momentum $p_z \equiv 2\pi\partial_+ v/g$ conjugate to z . With $\varphi_+ = \varphi_-^\dagger$ and imposing periodic boundary conditions (DLCQ), the remaining two fields are quantized canonically. It is justified [7] to restrict to the *fundamental modular domain* ($0 < z < 1$), in which they are represented by

$$\varphi_3(x^-) = \frac{a_0}{\sqrt{4\pi}} + \frac{1}{\sqrt{4\pi}} \sum_{n=1}^{\infty} \left(a_n w_n e^{-in\frac{\pi}{L}x^-} + a_n^\dagger w_n e^{+in\frac{\pi}{L}x^-} \right), \quad (5)$$

$$\text{and} \quad \varphi_-(x^-) = \frac{e^{+i\frac{\pi}{2L}x^-}}{\sqrt{4\pi}} \sum_{m=\frac{1}{2}}^{\infty} \left(b_m u_m e^{-im\frac{\pi}{L}x^-} + d_m^\dagger v_m e^{+im\frac{\pi}{L}x^-} \right). \quad (6)$$

The single particle operators a_n , b_m and d_m are the carriers of the operator structure and obey conventional commutator relations like $[a_n, a_{n'}^\dagger] = \delta_{n,n'}$ and $[b_m, b_{m'}^\dagger] = [d_m, d_{m'}^\dagger] = \delta_{m,m'}$ with all others vanishing except those involving the zero mode a_0 . The coefficients

$$w_n = 1/\sqrt{n}, \quad u_m = 1/\sqrt{m+\zeta}, \quad \text{and} \quad v_m = 1/\sqrt{m-\zeta}, \quad \text{with} \quad \zeta \equiv z - \frac{1}{2}, \quad (7)$$

are real and depend on the vector potential v through ζ . It is justified to think of the ‘a’-, ‘b’-, and ‘d’-particles as of photons, electrons, and positrons, except that they are all bosons. Below, use of this will be made both in the notation and the diagrammatical representation.

Neither a_0 , the zero mode of φ_3 , nor the remaining three fields A_3^- , A_-^- and A_+^- have a conjugate momentum. They cannot be quantized canonically but determine themselves by certain equations of motion. The A_a^- are determined by the three Gauss’ equations. In terms of the current

$$\mathbf{J}^\beta = \frac{1}{i} [\Phi, \mathbf{D}^\beta \Phi] \quad (8)$$

and its density components $J_a^+ = 2\text{Tr}(\tau^a \mathbf{J}^+)$ they read as

$$-\partial_-^2 A_3^- = gJ_3^+, \quad -(\partial_- + igv)^2 A_+^- = gJ_+^+, \quad \text{and} \quad -(\partial_- - igv)^2 A_-^- = gJ_-^+. \quad (9)$$

The first of them can be solved only if the zero mode [7] of the r.h.s

$$\langle J_3^+ \rangle_0 \equiv \frac{1}{2L} \int_{-L}^L dx^- J_3^+(x^-), \quad \text{thus} \quad Q_3 = 2L \langle J_3^+ \rangle_0 = \sum_{m=\frac{1}{2}}^{\infty} (d_m^\dagger d_m - b_m^\dagger b_m), \quad (10)$$

vanishes. This cannot be satisfied as an operator, but must be used to select out physical states. To find them is easy: they must have the same total number of ‘b’ and ‘d’ particles. When discussing below the spectra we will see, that this condition is different from the naive picture of color singlets. Finally, one must express a_0 in terms of the independent fields. The defining *constraint equation* is linear in a_0 , for details see Ref.[7]. In the solution, a_0 should be an explicit functional of the Fock-space operators, and a function of ζ and μ , *i.e.*

$$a_0 \equiv a_0 [a_n^\dagger, b_m^\dagger, d_m^\dagger, a_n, b_m, d_m; \zeta, \mu]. \quad (11)$$

Thus far, only approximate solutions have been constructed [8].

3 On the Hamiltonian and its Diagonalization

Upon evaluation [7], the total (light-cone) momentum P^+ becomes a diagonal and thus simple Fock-space operator

$$P^+ = \frac{\pi}{L} \sum_{n=1}^{\infty} n a_n^\dagger a_n + \frac{\pi}{L} \sum_{m=\frac{1}{2}}^{\infty} \left[(m + \zeta) b_m^\dagger b_m + (m - \zeta) d_m^\dagger d_m \right]. \quad (12)$$

The total (light-cone) energy P^- , the ‘Hamiltonian’ of the theory, is a off-diagonal Fock-space operator [7]. It is so complicated that we only outline its construction and refer for details to [7].

The defining equation is with $\hat{g} \equiv g/\sqrt{16\pi}$

$$\begin{aligned} P^- &= -4\hat{g}^2 \frac{L}{\pi} \frac{d^2}{dz^2} + \frac{1}{2} \int_{-L}^{+L} dx^- \left(\mu_0^2 (\phi_3 \phi_3 + \phi_+ \phi_- + \phi_- \phi_+) + \partial_- A_3^- \partial_- A_3^- \right) \\ &+ \frac{1}{2} \int_{-L}^{+L} dx^- \left((\partial_- + igv) A_+^- (\partial_- - igv) A_-^- + (\partial_- - igv) A_-^- (\partial_- + igv) A_+^- \right). \end{aligned} \quad (13)$$

To get it as a Fock-space operator one expresses the charge densities of Eq.(8) in terms of the ϕ_a and substitutes Eqs. (5) and (6). Inverting Eqs.(9) yields A_a^- in terms of the Fock-space operators and of a_0 , thus [7]

$$P^- = P^- \left[a_0; a_n^\dagger, b_m^\dagger, d_m^\dagger, a_n, b_m, d_m; \zeta, \mu \right]. \quad (14)$$

Finally, one has to invert the constraint equation for a_0 and to substitute Eq.(11) everywhere. As a results one gets the Hamiltonian in terms of ‘raw-ordered’ Fock-space operator products. It is reasonable to rewrite these ‘time ordered products’ as normal ordered products plus the sum of all pairwise contractions. The totally contracted terms are identical with the Fock-space vacuum expectation value which we conveniently define as $W(\zeta) \equiv \langle 0 | P^- | 0 \rangle$. Contrary to conventional DLCQ these may not be discarded since as functions of ζ they are part of the operator structure. Terms with one creation and one destruction operator are usually referred to as the ‘contraction terms’ or the ‘self-induced inertias’ P_C^- , those with two creation and two destruction operators as ‘seagulls’ P_S^- , those with one creation and three destruction operators as ‘forks’ P_F^- . Explicit formulas can be found in Appendices A, B, and C, respectively. They have been derived for $a_0 = 0$, but one should emphasize that a non-vanishing a_0 contributes to the ‘gauge potential energy’ $W(\zeta)$ as well as to the contractions, seagulls and forks. In general, the Hamiltonian becomes thus

$$P^- = -4\hat{g}^2 \frac{L}{\pi} \frac{d^2}{d\zeta^2} + W(\zeta) + P_C^-(\zeta) + P_S^-(\zeta) + P_F^-(\zeta). \quad (15)$$

In principle one has to diagonalize simultaneously momentum, energy and charge, *i.e.*

$$P^+ |\Psi_i\rangle = P_i^+ |\Psi_i\rangle , \quad P^- |\Psi_i\rangle = P_i^- |\Psi_i\rangle , \quad \text{and} \quad Q_3 |\Psi_i\rangle = 0 , \quad (16)$$

repectively. The denumerable eigenvalues of momentum and energy are denoted by P_i^+ and P_i^- , respectively. For the momentum and the charge this is not difficult, since any arbitrary Fock state

$$|\nu\rangle = a_{n_1}^\dagger a_{n_2}^\dagger \dots b_{m_1}^\dagger b_{m_2}^\dagger \dots d_{p_1}^\dagger d_{p_2}^\dagger \dots |0\rangle \quad (17)$$

with the same number of b- and d-particles is a solution, labelled appropriately by $\nu = 1, 2, \dots, N$. The number of states N is finite for any fixed value of the ‘harmonic resolution’ [3] $K \equiv LP_i^+/\pi$. Since energy and momentum commute, they span a complete set of states for diagonalizing the energy. The Fock space vacuum $|0\rangle$, defined by

$$a_n |0\rangle = 0 , b_m |0\rangle = 0 , \quad \text{and} \quad d_m |0\rangle = 0 , \quad (18)$$

has no particle content and thus vanishing momentum.

Next to being an operator in Fock space the Hamiltonian is a Schrödinger operator with respect to the gauge field v or ζ . Generating a complete set of functions $\psi_n(\zeta)$ by solving a Schrödinger equation with a convenient single particle potential $V(\zeta)$,

$$\left(-4\hat{g}^2 \frac{d^2}{d\zeta^2} + V(\zeta)\right)\psi_n(\zeta) = \omega_n \psi_n(\zeta) , \quad (19)$$

the solutions to Eq.(16) *must have a non-separable structure, i.e.*

$$|\Psi_i\rangle = \sum_{n=0}^{\infty} \sum_{\nu=1}^N C_{n,\nu}^{(i)} \psi_n(\zeta) |\nu\rangle , \quad \text{with} \quad C_{n,\nu}^{(i)} \neq c_n^{(i)} c_\nu^{(i)} . \quad (20)$$

This statement holds in general, since the coefficient functions of the Fock-space operators in the Hamiltonian depend on ζ in a complicated way. The physical vacuum $|vac\rangle$ that is the state with lowest energy of the full theory will thus acquire structure with respect to ζ as in [7], see also [8], entirely due to a ‘physical gauge’ like $\partial_- \mathbf{A}^+ = 0$ as opposed to the ‘light-cone gauge’ $\mathbf{A}^+ = 0$. But these structures will be disregarded in the rest of the paper where the vacuum is simple due to the model assumptions.

4 The Model within the Model

In the present work we approach the problem from the tail. We are interested in the particle sector, its spectral properties and wavefunctions. As a first step, in order to face a tractable problem, we

do *not neglect* but *omit by hand* a_0 , and in addition suppress the fluctuations in the gauge mode, *i.e.*

$$a_0 \equiv 0 \quad \text{and} \quad \psi_n(\zeta) \equiv \delta_{n,0} \delta(\zeta) , \quad (21)$$

see also Ref.[7]. For $\zeta \equiv 0$ the Hamiltonian becomes then

$$P^- = P_{\text{Fock}}^- \equiv P_C^- (0) + P_S^- (0) + P_F^- (0) . \quad (22)$$

One should emphasize that this model does *not correspond* to the light-cone gauge since we keep $gvL = \pi/2$ as the static value around which the dynamic treatment would fluctuate. Last not least, we perform a Tamm-Dancoff truncation by restricting to the lowest, the 2-particle sectors. This ‘model within the model’ will provide useful insight into the structure of the full solution.

The ‘contraction terms’ P_C^- as given in Appendix A should deserve some explanatory remarks. In a first step one gets for them rather straightforwardly

$$\frac{\pi}{L} P_C^- = \sum_{n=1}^{\infty} \frac{I_n(\zeta)}{n} a_n^\dagger a_n + \sum_{m=\frac{1}{2}}^{\infty} \frac{J_m(+\zeta)}{m+\zeta} b_m^\dagger b_m + \sum_{m=\frac{1}{2}}^{\infty} \frac{J_m(-\zeta)}{m-\zeta} d_m^\dagger d_m . \quad (23)$$

The ‘self-induced inertias’ or ‘tadpole diagrams’ I and J contain logarithmically diverging pieces,

$$I_n(\zeta) = \mu_0^2 + \hat{g}^2 \sum_{m=\frac{1}{2}}^{\infty} \left[\frac{2}{(m+\zeta)} + \frac{4n}{(m-n+\zeta)^2} - \frac{4n}{(m+n+\zeta)^2} \right. \\ \left. + \frac{2}{(m-\zeta)} + \frac{4n}{(m-n-\zeta)^2} - \frac{4n}{(m+n-\zeta)^2} \right] , \quad (24)$$

$$J_m(\zeta) = \mu_0^2 + \hat{g}^2 \sum_{n=1}^{\infty} \left[\frac{2}{n} + \frac{4(m+\zeta)}{(m-n+\zeta)^2} - \frac{4(m+\zeta)}{(m+n+\zeta)^2} \right] \\ + \hat{g}^2 \sum_{p=\frac{1}{2}}^{\infty} \left[\frac{1}{(p-\zeta)} + \frac{1}{(p+\zeta)} + \frac{4(m+\zeta)}{(m-p)^2} - \frac{4(m+\zeta)}{(m+p)^2} \right] , \quad (25)$$

through terms like $\sum_{n=1}^{\infty} 1/n$. They can be cancelled by renormalizing the mass like

$$\mu_0^2 = \mu^2 - 16\hat{g}^2 - 2\hat{g}^2 \left(\sum_{m=\frac{1}{2}}^{\infty} \frac{1}{m} + \sum_{n=1}^{\infty} \frac{1}{n} \right) = \mu^2 - (16+C)\hat{g}^2 - 4\hat{g}^2 \sum_{m=1}^{\infty} \frac{1}{m} , \quad (26)$$

with $\hat{g} = g/\sqrt{16\pi}$. Important is that the renormalized mass μ is *finite*. Its value is not unique, and thus both the ‘16’ and the constant

$$C \equiv 2 \sum_{m=\frac{1}{2}}^{\infty} \frac{1}{m} - 2 \sum_{n=1}^{\infty} \frac{1}{n} = 4 \ln 2 \quad (27)$$

could be absorbed into the renormalized μ . But here is the problem: The sums in Eqs. (24) and (25) are not completely symmetric in the integers and half-integers. Converting the expressions tabulated in Table 1 generates the constant C in either one place or the other. In the continuum limit the two sums in Eq.(27) tend to cancel in line with Section 6. We therefore shall work with $C = 0$ whenever not mentioned otherwise.

5 Numerical Solutions

Consider two types of 2-particle Fock states, referred to as the ‘aa’- and the ‘bd’-space, respectively,

$$\begin{aligned} |n\rangle_a &= a_n^\dagger a_{K-n}^\dagger |0\rangle \quad \text{for } n = 1, \dots, \left[\frac{K}{2}\right], \\ \text{and } |m\rangle_b &= b_m^\dagger d_{K-m}^\dagger |0\rangle \quad \text{for } m = \frac{1}{2}, \dots, K - \frac{1}{2}. \end{aligned} \quad (28)$$

They are orthogonal, $\langle m|n\rangle = 0$, and simultaneous eigenstates of Q_3 and P^+ , *i.e.*

$$Q_3 |n\rangle_a = 0 \quad , \quad P^+ |n\rangle_a = \frac{\pi}{L} K |n\rangle_a \quad , \quad (29)$$

$$Q_3 |m\rangle_b = 0 \quad , \quad P^+ |m\rangle_b = \frac{\pi}{L} K |m\rangle_b \quad , \quad (30)$$

for all values of n and m , as they should according to Eq.(16). Gauss’ equation (9) prevents us from including also ‘charged’ states like for example $b_m^\dagger a_{K-m}^\dagger |0\rangle$. Any of the $K + [K/2]$ linear superposition of these basis states like

$$|\Psi_i\rangle = \sum_{n=1}^{\left[\frac{K}{2}\right]} \langle n | \tilde{C}_a | i \rangle |n\rangle_a + \sum_{m=\frac{1}{2}}^{K-\frac{1}{2}} \langle m | \tilde{C}_b | i \rangle |m\rangle_b = \sum_{n=1}^{\left[\frac{K}{2}\right]} \langle n | \Psi_{i,a} \rangle |n\rangle_a + \sum_{m=\frac{1}{2}}^{K-\frac{1}{2}} \langle m | \Psi_{i,b} \rangle |m\rangle_b \quad (31)$$

are thus eigenfunctions of Q_3 and P^+ with the same eigenvalues, while the unitary matrix $U = \tilde{C}_a + \tilde{C}_b$ determines itself by diagonalizing P^- , with the $(K + [K/2])$ eigenvalues P_i^- and subject to normalization

$$\langle i | U^\dagger U | i \rangle = 1, \quad \text{for all } i. \quad (32)$$

Since $P^\nu P_\nu = 2P^+P^-$ is to be interpreted as the operator of invariant mass squared M^2 , the eigenvalues of P^- will be presented below as the product $2P_i^+P_i^- \equiv M_i^2$. As unit of mass we shall use $m_u = \hat{g} = g/\sqrt{16\pi}$. Note that the coupling constant g has here the dimension of a mass.

As a rather welcome advantage of a DLCQ calculation, the diagonalization of 100×100 matrices takes only a couple of milliseconds on a modern work station. One thus could go to fairly large

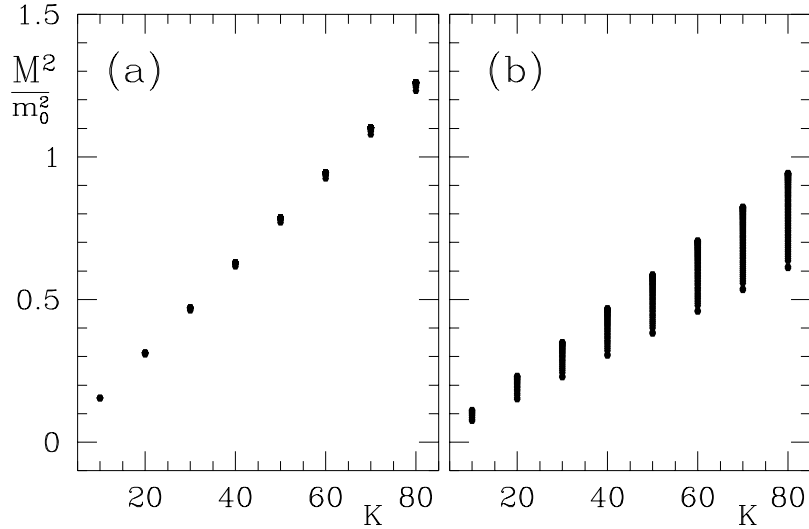


Figure 1: *Invariant mass squared eigenvalues M_i^2 versus Harmonic Resolution K .* – Left side (a): *The Fock space is restricted to only the aa-states $|n\rangle_a$.* Note the almost complete degeneracy of all $K/2$ states. Right side (b): *The Fock space is restricted to only the bd-states $|n\rangle_b$.* – Note: *All eigenvalues increase roughly linear in K , and show no trend to stabilize.* – Parameters values are $\mu^2 = 0$ and $m_0^2 = 2(100m_u)^2$.

values of the resolution within our simple model. However, in order to unravel the structure of the spectra and not to be overwhelmed by a flood of data, we first keep the mass parameter fixed to $\mu = 0$ and restrict ourselves to $20 \leq K \leq 80$. In view of typical values for the harmonic resolution $K \leq 22$ quoted in the literature [10, 11, 12, 13] the above range is still large for practical purposes.

1. The reduced 2-particle Fock spaces. When one restricts to *only* the aa-space, the Hamiltonian matrix $\langle n' | P^- | n \rangle$ is diagonal from the outset, since the a-particles have no interaction according to Table 2. They only have self-induced inertias. To first order of approximation, for moderately small values of μ these inertias are linear in the momentum. The eigenvalues of P^- become approximately independent of K and thus the invariant masses therefore linear in K and highly degenerate, as displayed in Figure 1a as function of K .

If one restricts oneself to *only* the bd-space, the Hamiltonian matrix is non-diagonal due to the interaction between the b- and the d-particles. As displayed in Figure 1b, this causes the eigenvalues

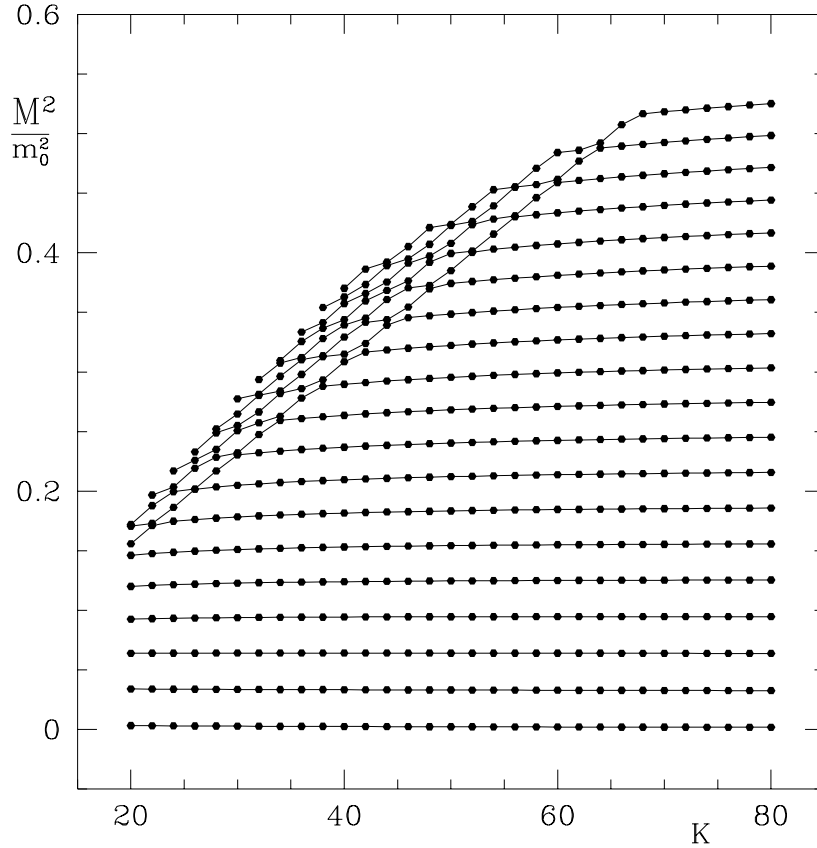


Figure 2: *Invariant mass squared eigenvalues M_i^2 versus Harmonic Resolution K . – The Fock space includes both the aa - and bd -states. Note: The lowest eigenvalues M_i^2 are roughly independent of K , with a roughly constant spacing. – Parameters values are $\mu^2 = 0$ and $m_0^2 = 2(100m_u)^2$.*

to spread over a wider range of energies but obviously not strong enough so as to stabilize the low energy parts of the spectrum. One understands this behaviour analytically, see Section 6.

2. The 2-particle Fock space. The behaviour changes drastically if one includes simultaneously the aa - and the bd -states. One now allows for the virtual scattering from the aa -space into the bd -space and back, represented by the matrix elements $S_{aa}(n_1, n_2; n_3, n_4)$ in Table 2. In Figure 2, the first 19 mass squared eigenvalues are plotted as functions of K . At a first glance the eigenvalues are K -independent, with a roughly equal spacing like the states in a harmonic oscillator well. At the left upper corner of the figure seem to develop some ‘crossings’ of the states, which we shall resolve and explain below. At a second glance, the spacing is not completely independent of the energy, rather it decreases slowly with increasing energy, typically like the eigenstates in a potential with linearly increasing walls.

We like to emphasize the discreteness of the spectrum. Discreteness surviving the continuum limit $K \rightarrow \infty$ should be considered as the earmark of confinement, even if such a statement seems premature within the present 1+1 dimensional ‘model within a model’. Most if not all field theories particularly QED confine in 1+1 dimension [15, 16]. Remarkable however is that one gets such a spectrum at all, in a model with no other ingredients than pure gauge theory.

A word of caution seems in order. The restriction to the 2-particle sector is *ad hoc* and should not be overemphasized. Including more and more particles, one would expect structures which would tend to true continua for ever increasing K . At least parts of the so obtained spectra would correspond to ‘physical glue-balls in relative motion’. In short and over-stressing the point, one would expect spectra which qualitatively resemble the multi-particle spectra of QED in (1+1) dimensions, as displayed in the figures of Ref.[15, 16].

3. Symmetries and Multiplet structure. In the naive thinking of color invariance a color singlet should have a finite spectrum. Are our eigenstates color singlets? Opposed to this interpretation is that the spectrum diverges when restricting to either aa- or bd-states *alone* as displayed in Figure 1. Only when both are included, one has a chance for having wave functions which are invariant under rotations in color space. Can one be more specific? What are the *symmetries* of our problem?

By inspecting the numerical results for the eigenfunctions one observes three distinctly different classes: (I) those with $\Psi_{i,a} \sim \Psi_{i,b}$, (II) those with $\Psi_{i,a} \sim 0$, and (III) those with $\Psi_{i,a} \sim -2\Psi_{i,b}$, for comparable size of the single particle momenta. A separation into two groups can be based on an exact symmetry: the Hamiltonian is invariant when exchanging the b- and the d-particles. Denoting the corresponding charge-conjugation operator by C_π , its eigenvalues must be $C'_\pi = \pm 1$. In fact *all* numerical eigenfunctions are *either* charge-conjugation even *or* odd, by inspection, and the latter coincides with the class II states. Aiming at a measure to classify the states we introduce the operators

$$Q_- = \sum_{n=1}^{\infty} a_n^\dagger b_{n+\frac{1}{2}} - a_n d_{n-\frac{1}{2}}^\dagger, \quad Q_+ = \sum_{n=1}^{\infty} a_n b_{n+\frac{1}{2}}^\dagger - a_n^\dagger d_{n-\frac{1}{2}}. \quad (33)$$

Together with Q_3 they satisfy SU(2) commutation relations in the Weyl representation

$$[Q_3, Q_-] = Q_-, \quad [Q_+, Q_3] = Q_+, \quad [Q_-, Q_+] = Q_3, \quad (34)$$

with the group invariant

$$Q^2 \equiv Q_3 Q_3 + Q_- Q_+ + Q_+ Q_- . \quad (35)$$

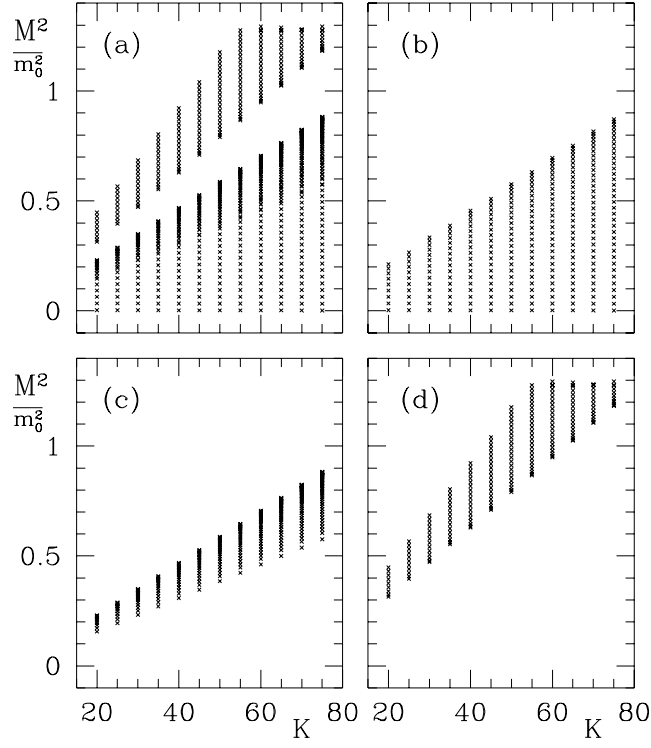


Figure 3: *Spectral Decomposition with Multiplet Q .* – For each state $|i, K\rangle$ the multiplet expectation value Q is calculated, and the spectrum disentangled correspondingly, see text. – Upper left (a): Full spectrum. Upper right (b): Spectrum of the quasi-singlets ($Q = 0$). Lower left (c): Spectrum of the quasi-triplets ($Q = 1$). Lower right (d): Spectrum of the quasi-pentuplets ($Q = 2$). – Note: Only the singlet states have a stable spectrum. – Parameters values are $\mu^2 = 0$ and $m_0^2 = 2(100m_u)^2$.

The eigenfunctions of the Hamiltonian cannot be eigenfunctions to Q^2 since the two do not commute, see also Section 7 below. One can however calculate the *expectation values* $q_i \equiv \langle \Psi_i | Q^2 | \Psi_i \rangle$. The ‘effective eigenvalues’ Q_e , defined by $Q_e(Q_e + 1) = q_i$, turn out to be close to the numbers $0, 1, 2, \dots$. We therefore define

$$Q = \begin{cases} 0, & \text{if } 0.0 < Q_e < 0.3 \text{ (class I);} \\ 1, & \text{if } 0.7 < Q_e < 1.3 \text{ (class II);} \\ 2, & \text{if } 1.7 < Q_e < 2.3 \text{ (class III).} \end{cases} \quad (36)$$

It is remarkable, that none of the expectation values drops out of the comparably narrow limits set in these equations. Is this a consequence of a residual symmetry in the Hamiltonian? – For 2 particles the largest possible value is $Q = 2$. As it turns out, all numerical eigenstates have a charge-conjugation parity $C'_\pi = (-1)^Q$, particularly the triplet is charge-conjugation odd. In

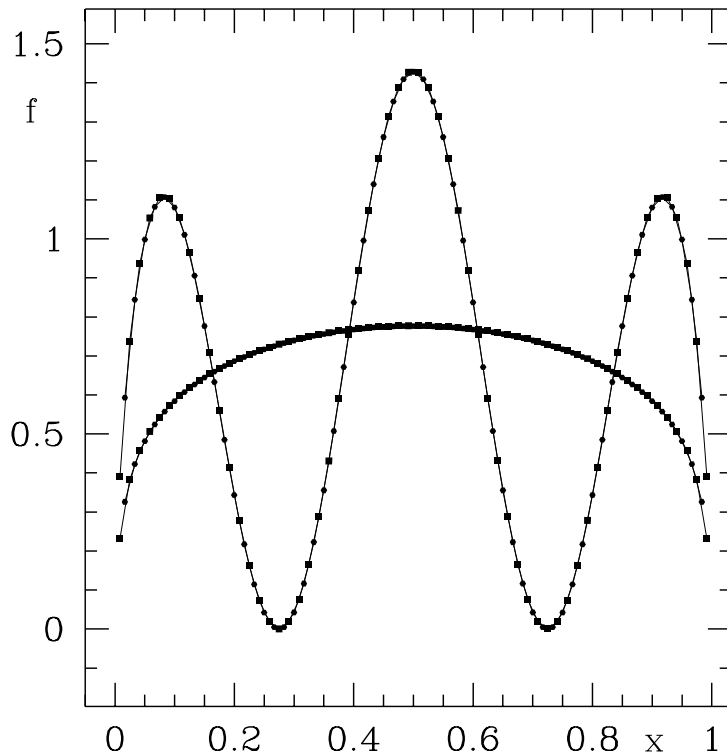


Figure 4: *Structure Functions versus Momentum Fraction x .* – The structure function is calculated both for the a - and the b -particles, ($x \equiv n/K$, squares) and ($x \equiv m/K$, bullets), respectively, for the ground and the first excited state. – Note: The curve interpolating between squares and bullets is remarkably smooth. Note also, that the structure function of the excited state has more nodes than the one of the ground state, in accord with expectation. – Parameters values are $\mu^2 = 0$ and $K = 60$.

Figure 3 the same spectrum as in Figure 2 is displayed, but separated according to the multiplet-value Q . As it turns out, the crossing situation mentioned in the context of Figure 2 is due to the crossing between $Q = 0$ and $Q = 1$ states. *All* eigenvalues of the singlet $Q = 0$ become virtually *independent* of the resolution. As opposed to this *all* members of the triplets or pentuplets, $Q = 1$ or $Q = 2$, respectively, are at least linear in K , tending to infinity in the continuum limit.

The latter result is remarkable since it is one of the few direct evidences that only singlets can have finite masses in a non-abelian theory. Some subtleties related to this interpretation will be discussed further below in Section 7.

4. Structure Functions. Next to the spectrum we investigate explicitly the eigenfunctions. Due to diagonalization one knows them for all eigenstates, particularly their projections on the Hilbert

space, $\langle n|\Psi_i\rangle = \langle n|\tilde{C}_a|i\rangle$ and $\langle m|\Psi_i\rangle = \langle m|\tilde{C}_b|i\rangle$, see also Eq.(31). The probabilities to find an a- or a b-particle with longitudinal momentum $p^+ = n\frac{\pi}{L}$ or $p^+ = m\frac{\pi}{L}$ are given by

$$\langle \Psi_i | a_n^\dagger a_n | \Psi_i \rangle = \langle n | \tilde{C}_a | i \rangle^2, \quad \text{and} \quad \langle \Psi_i | b_m^\dagger b_m | \Psi_i \rangle = \langle m | \tilde{C}_b | i \rangle^2, \quad (37)$$

repectively, and are related to the structure functions $f(x)$ by

$$f_i^{(a)}(n/K) = K \langle \Psi_i | a_n^\dagger a_n | \Psi_i \rangle, \quad \text{and} \quad f_i^{(b)}(m/K) = K \langle \Psi_i | b_m^\dagger b_m | \Psi_i \rangle. \quad (38)$$

In the continuum, the probability to find a parton with longitudinal momentum fraction between $x = n/k$ and $x + dx$ is $dx f(x)$. Note that the structure functions are *not* normalized to unity, because of Eq.(32), rather they obey the *sum rule* $\int_0^1 dx \left(\frac{1}{2} f_i^{(a)}(x) + f_i^{(b)}(x) \right) = 1$. In displaying them in Figure 4, we restrict ourselves to the first two states. Due to the residual SU(2) symmetry the structure functions for the a- and b-particles turn out to be extremely similar, for which reason they have been compiled in the same plot. By inspection the structure function for the first state can be approximated by

$$f_\alpha(x) = \frac{2}{3} \frac{\Gamma(2 + 2\alpha)}{[\Gamma(1 + \alpha)]^2} [x(1 - x)]^\alpha, \quad (39)$$

with an exponent numerically closer to $\alpha \sim \frac{1}{3}$ than to $\alpha \sim \frac{1}{4}$. All higher states have more nodal structures.

5. Mass-Dependence. The results presented thus far have been calculated for a vanishing value of the mass parameter μ . For a mass parameter μ much larger than the effective coupling constant \hat{g} one can omit the interaction to first order of approximation. With increasing μ , the spectrum must become more and more like the one of two free massive bosons, that is like $\sim \frac{\mu^2}{x(1-x)}$. Correspondingly, the structure function of the lowest state will be peaked at $x = 1/2$ with an ever decreasing width like a δ -function. As shown in Figure 5, this is exactly what happens. Keeping \hat{g} fixed and increasing μ the spectrum changes from being ‘interaction dominated’ at $\mu \sim 0$ in the manner as having been shown in Figure 2 to being ‘mass dominated’ beyond $\mu \sim 100m_u$. A good earmark of the latter is the decreasing level density with increasing excitation.

6. Does the Continuum Limit exist? The spectra shown in Figs. 2 and 3 for $20 \leq K \leq 80$ did appear to be stable as function of K . Are they really? What happens when one increases K by order of magnitudes? Does the continuum limit exist? – The question can be answered either analytically by converting the Hamiltonian matrix equation to an integral equation, or numerically by increasing the *order of magnitude* of K . We have done both. The continuum limit is discussed

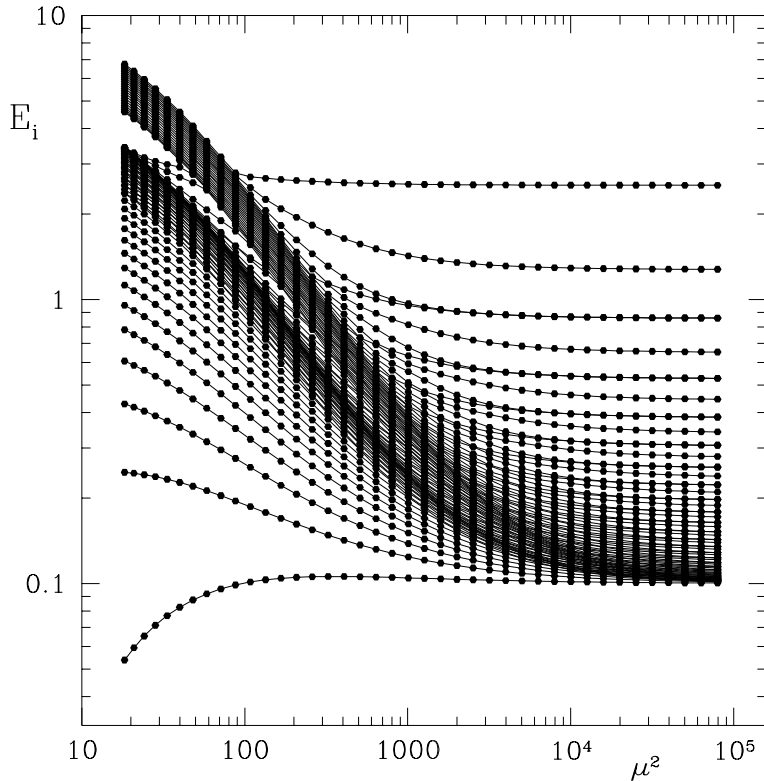


Figure 5: Invariant mass squared eigenvalues $E_i = 2M_i^2/(1000m_u^2 + 40\mu^2)$ versus Mass Parameter μ^2 . Note the logarithmic scale and how the spectrum changes from being ‘interaction dominated’ at smaller to being ‘mass dominated’ at larger values of μ . – The harmonic resolution is fixed at $K = 50$.

in detail in Section 6. Here we present the numerical results, by varying K up to $K \sim 1000$. Plotting the results in Figure 6 on a logarithmic scale one is able to unravel logarithmically small variations which skip the observation on a linear scale. The unexpectedly large but still modest variation of the eigenvalues with increasing resolution particularly their positive curvature seems to indicate convergence to the continuum limit, in line with the analytic considerations below in Section 6. We have verified this behaviour numerically also for larger values of the mass parameter μ , but renounce to display the results. For negative values of the mass parameter, however, *i.e.* for $\mu^2 < 0$ the eigenvalue curves tend to develop an increasingly strong negative curvature with respect to $\ln K$, again in line with analytic considerations.

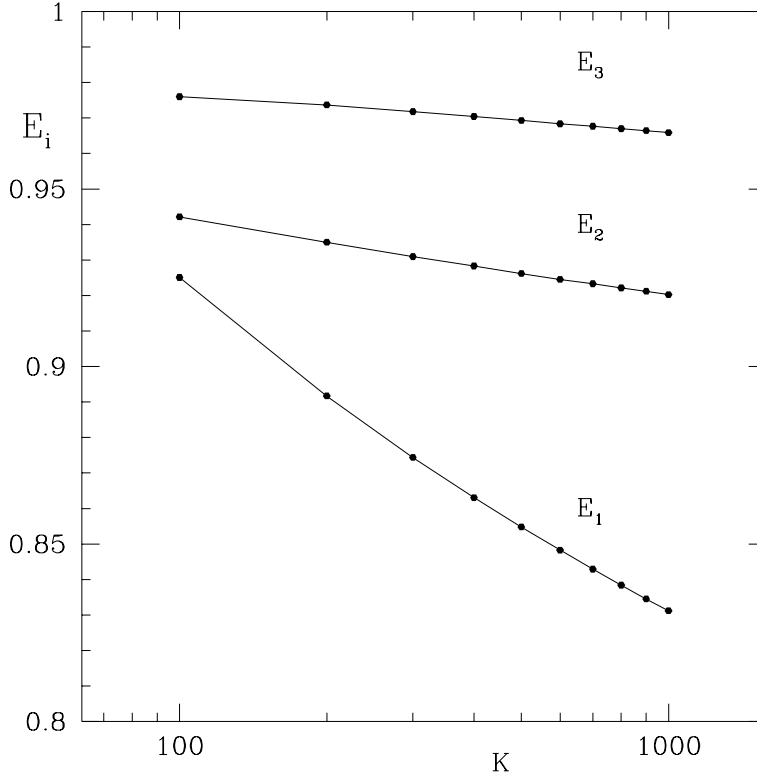


Figure 6: Eigenvalues E_i versus Large Harmonic Resolution K . – The lowest three eigenvalues are plotted in however different mass units $E_i = P_i^- P_i^+ / m_i^2$ with $m_1^2 = 75m_u^2$, $m_2^2 = 480m_u^2$, $m_3^2 = 730m_u^2$. They are reasonably but not completely stable and vary on a level of less than 10 per cent. They seem to converge in the continuum limit $K \rightarrow \infty$.

6 Coupled Integral Equations in the Continuum Limit

According to Eq.(28), one deals with orthogonal vector spaces $\langle m|n\rangle = 0$. In such a space the eigenvalue problem $P^- |\Psi_i\rangle = P_i^- |\Psi_i\rangle$ becomes a set of two coupled matrix equations, *i.e.*

$$\sum_{m'=\frac{1}{2}}^{K-\frac{1}{2}} \langle n|P^-|m'\rangle \langle m'|\Psi_i\rangle = \left(P_i^- - \langle n|P^-|n\rangle\right) \langle n|\Psi_i\rangle, \quad (40)$$

$$\sum_{n'=1}^{[K/2]} \langle m|P^-|n'\rangle \langle n'|\Psi_i\rangle + \sum_{m'=\frac{1}{2}}^{K-\frac{1}{2}} \langle m|P^-|m'\rangle \langle m'|\Psi_i\rangle = \left(P_i^- - \langle m|P^-|m\rangle\right) \langle m|\Psi_i\rangle, \quad (41)$$

see also Eq.(31). As mentioned, matrix elements like $\langle n|P^-|n'\rangle$ vanish in the present model. Hence forward we substitute $P_i^- = \omega_i/P_i^+$ and drop the index i . The notation accounts for the obvious fact that the off-diagonal matrix elements are calculated differently from the diagonal ones and

that the latter are taken to the r.h.s. of the equations. Correspondingly, in the continuum limit, one is confronted with a set of two *coupled integral equations*

$$\omega \psi_a(x) = I_a(x) \psi_a(x) + \int_0^1 dx' \langle x | K_a | x' \rangle \psi_b(x'), \quad (42)$$

$$\omega \psi_b(x) = I_b(x) \psi_b(x) + \int_0^1 dx' \langle x | K_b | x' \rangle \psi_b(x') + \int_0^{\frac{1}{2}} dx' \langle x | K_a | x' \rangle \psi_a(x'). \quad (43)$$

More specifically, the continuum limit is obtained by the limiting procedure $n \rightarrow \infty$ and $K \rightarrow \infty$ at *fixed momentum fractions* $x = n/K$, replacing sums by integrals like for example

$$\sum_{m'=\frac{1}{2}}^{K-\frac{1}{2}} F(m, m') = \int_0^1 dx' F(x, x'), \quad \text{with } F(x, x') \equiv K F(m, m'). \quad (44)$$

Care has to be taken of a proper removal of the ‘diagonal kernels’, *i.e.*

$$\int_0^1 dx' F(x, x') \equiv \int_0^{x-\epsilon} dx' F(x, x') + \int_{x+\epsilon}^1 dx' F(x, x'), \quad (45)$$

with the limit $\epsilon \rightarrow 0$ taken at the end. Matrix elements are thus related to kernels by

$$\langle x | K_a | x' \rangle = K P^+ \frac{\pi}{L} \langle n | P^- | m' \rangle, \quad \text{and} \quad \langle x | K_b | x' \rangle = K P^+ \frac{\pi}{L} \langle m | P^- | m' \rangle. \quad (46)$$

From Table 2 one gets

$$\langle x | K_a | x' \rangle = -\frac{2\hat{g}^2}{(x-x')^2} \frac{(x+x')(2-x-x')}{\sqrt{x(1-x)x'(1-x')}} - \frac{2\hat{g}^2}{(1-x-x')^2} \frac{(1+x-x')(1-x+x')}{\sqrt{x(1-x)x'(1-x')}}}, \quad (47)$$

$$\langle x | K_b | x' \rangle = -\frac{2\hat{g}^2}{(x-x')^2} \frac{(x+x')(2-x-x')}{\sqrt{x(1-x)x'(1-x')}} + 2\hat{g}^2 \frac{(1-2x)(1-2x')}{\sqrt{x(1-x)x'(1-x')}}}. \quad (48)$$

In the sequel the obvious symmetry $\langle x | K_a | x' \rangle = \langle x | K_a | 1-x' \rangle$ will be used without further mentioning. Note the non-integrable quadratic singularities at $x' = x$ and $x' = 1-x$. The wavefunctions become $\langle m | \Psi \rangle = \psi_a(x)$ and $\langle n | \Psi \rangle = \psi_b(x)$. The diagonal terms are obtained from Table 1, *i.e.*

$$I_a(x) = \frac{C\hat{g}^2}{x(1-x)} + I_b(x), \quad \text{and} \quad I_b(x) = \frac{\mu^2 + 16\hat{g}^2}{x(1-x)} + \int_0^1 \frac{16\hat{g}^2 dz}{(x-z)^2}. \quad (49)$$

We now seek the solution in the regime which corresponds to the color singlets, namely

$$\psi_b(x) = \psi_b(1-x) = \psi_a(x) \equiv \psi(x). \quad (50)$$

The coupled integral equations (42) and (43) degenerate then into two equations for one function

$$\omega \psi(x) = I_a(x) \psi(x) + \int_0^1 dx' \langle x | K_a | x' \rangle \psi(x'), \quad \text{and} \quad (51)$$

$$\omega \psi(x) = I_b(x) \psi(x) + \int_0^1 dx' \langle x | K_b | x' \rangle \psi(x') + \frac{1}{2} \int_0^1 dx' \langle x | K_a | x' \rangle \psi(x'). \quad (52)$$

One of them must therefore be redundant. To solve a singular equation like (51) one adds and subtracts a term like $I(x) = \int_0^1 dx' \langle x | K_a | x' \rangle$, *i.e.*

$$\omega \psi(x) = (I(x) + I_a(x)) \psi(x) + \int_0^1 dx' \langle x | K_a | x' \rangle (\psi(x') - \psi(x)) . \quad (53)$$

Close to the singularity, $\psi(x) - \psi(x') \sim x - x'$ converts the quadratic singularity into a pole which can be integrated by some principal value prescription. Now look at

$$I(x) + I_a(x) = \frac{\mu^2 + 16\hat{g}^2 + C\hat{g}^2}{x(1-x)} + 4\hat{g}^2 \int_0^1 \frac{dx'}{(x-x')^2} \left[4 - \frac{(x+x')(2-x-x')}{\sqrt{x(1-x)}\sqrt{x'(1-x')}} \right] . \quad (54)$$

Setting in the square bracket $x' = x + \Delta$ and expanding with Δ one notes that the first non-vanishing term is $\propto \Delta^2$. This cancels the singularity, and the integral becomes finite. The integral equation (51) has thus a solution. – As for Eq.(52) we subtract the latter from the former to get

$$\frac{C\hat{g}^2}{x(1-x)} \psi(x) = \int_0^1 dx' \psi(x') \left[\langle x | K_b | x' \rangle - \frac{1}{2} \langle x | K_a | x' \rangle \right] . \quad (55)$$

Inserting the kernels from Eqs. (47) and (48) the singular terms cancel precisely. One remains with

$$\frac{C\hat{g}^2}{x(1-x)} \psi(x) = 2\hat{g}^2 \frac{(1-2x)}{\sqrt{x(1-x)}} \int_0^1 dx' \psi(x') \frac{(1-2x')}{\sqrt{x'(1-x')}} = 0 , \quad (56)$$

because the integrand is an odd function around $x' = \frac{1}{2}$. One has to conclude: The second integral equation is consistent with the first one iff $C = 0$. Otherwise the continuum limit does not exist. This is in line also with the statement from color invariance: All three particles should have the same mass, see Eq.(49). – One remains with Eq.(51) which units adjusted is identical with the one of Bardeen *et al.* [17] and of Klebanov *et al.* [11], although the latter had been derived in another, *i.e.* in the light-cone gauge. We refer to their work particularly with respect to the endpoint analysis of the solutions.

7 Charge Conservation and Color Singlets

We take the multiplet structure of the spectra in Section 5 as kind of an empirical fact, and wonder whether they can be put on more solid grounds. This turns out more difficult than anticipated. – Of course, one always can associate charges with the currents as defined in Section 5, particularly $Q_- = \int dx^- J_-^+$, $Q_+ = Q_-^\dagger$, and the familiar Q_3 . Upon evaluation they become

$$Q_3 = \sum_{m=\frac{1}{2}}^{\infty} d_m^\dagger d_m - b_m^\dagger b_m , \quad \text{and} \quad Q_- = A_0 \left(a_0 b_{\frac{1}{2}} \right)_s + \sum_{n=1}^{\infty} A_n a_n^\dagger b_{n+\frac{1}{2}} - B_n a_n d_{n-\frac{1}{2}}^\dagger , \quad (57)$$

with $(a_0 b_{\frac{1}{2}})_s \equiv \frac{1}{2}(a_0 b_{\frac{1}{2}} + b_{\frac{1}{2}} a_0)$. In the fundamental modular domain the coefficients are

$$A_0 = \frac{1}{2}\sqrt{z}, \quad A_n = \frac{1}{2} \left(\sqrt{\frac{n+z}{n}} + \sqrt{\frac{n}{n+z}} \right), \quad \text{and} \quad B_n = \frac{1}{2} \left(\sqrt{\frac{n-z}{n}} + \sqrt{\frac{n}{n-z}} \right). \quad (58)$$

Since $[a_0, Q_3] = 0$, see Ref.[8], one calculates the SU(2)-commutators as follows:

$$\left[Q_3, Q_- \right] = Q_- \quad \text{and} \quad \left[Q_-, Q_+ \right] - Q_3 = \Delta(z, a_0). \quad (59)$$

The right hand side of this equation turns out to be

$$\begin{aligned} \frac{4}{z}\Delta(z, a_0) &\equiv \left[(a_0 b_{\frac{1}{2}})_s, (a_0 b_{\frac{1}{2}}^\dagger)_s \right] + \\ &+ \frac{2}{\sqrt{z}} \left[(a_0 b_{\frac{1}{2}})_s, \sum_{n=1}^{\infty} A_n a_n^\dagger b_{n+\frac{1}{2}} - B_n a_n d_{n-\frac{1}{2}}^\dagger \right] - \frac{2}{\sqrt{z}} \left[(a_0 b_{\frac{1}{2}}^\dagger)_s, \sum_{n=1}^{\infty} A_n a_n b_{n+\frac{1}{2}}^\dagger - B_n a_n^\dagger d_{n-\frac{1}{2}} \right] \\ &+ \sum_{n=1}^{\infty} \frac{z}{n^2 - z^2} \left(d_{n-\frac{1}{2}}^\dagger d_{n-\frac{1}{2}} - b_{n+\frac{1}{2}}^\dagger b_{n+\frac{1}{2}} \right) + \sum_{n=1}^{\infty} \frac{z^2}{n(n^2 - z^2)} \left(d_{n-\frac{1}{2}}^\dagger d_{n-\frac{1}{2}} + b_{n+\frac{1}{2}}^\dagger b_{n+\frac{1}{2}} + a_n^\dagger a_n \right) \end{aligned} \quad (60)$$

In passing one notes that the charges of Eq.(33) agree with those of Eq.(57) for $z = 0$ (thus $\Delta = 0$), and for $a_0 = 0$. Can one anticipate for the general case that $\Delta(z, a_0) = 0$? – One has two perspectives for the future: Either (I) the explicit solution for a_0 renders $\Delta = 0$, or (II) one requires $\Delta = 0$ as a subsidiary condition for solving a_0 . Here the matter rests as long as one cannot solve explicitly for a_0 .

But in either case seems to be a problem: The charges as defined by Eq.(57) cannot be conserved since $\partial_\beta \mathbf{J}^\beta \neq 0$. True, our model has a conserved four-current $\partial_\beta \tilde{\mathbf{J}}^\beta = 0$, since this follows directly from the color-Maxwell equations $\partial_\alpha \mathbf{F}^{\alpha\beta} = g \tilde{\mathbf{J}}^\beta$. But the two currents are not identical since $\tilde{\mathbf{J}}^\beta = \mathbf{J}^\beta + \frac{1}{i} [\mathbf{F}^{\beta\alpha}, \mathbf{A}_\alpha]$. Only for the latter holds

$$\frac{d}{dx^+} \tilde{\mathbf{Q}} = 0, \quad \text{with} \quad \tilde{\mathbf{Q}} = \int_{-L}^{+L} dx^- \tilde{\mathbf{J}}^+. \quad (61)$$

Thus $\tilde{\mathbf{Q}} = \mathbf{Q} + 2iL[\partial_+ \mathbf{A}^+, \mathbf{A}^+] + 2Lg[[\mathbf{A}^+, \langle \mathbf{A}^- \rangle_0], \mathbf{A}^+]$, or

$$\tilde{Q}_3 = Q_3, \quad \text{and} \quad \tilde{Q}_- = Q_- - 2Lgv^2 \langle A_+^- \rangle_0. \quad (62)$$

But now, in the process of inverting the Gauss' equations (9), their zero modes have been required to vanish [7]. This in turn leads to $\tilde{Q}_\pm \equiv 0$, in total and unpleasant opposition to tribal beliefs that the true and dynamically conserved charges \tilde{Q}_a obey a non-Abelian group structure.

As a possible way out we proffer a different gauge choice namely

$$\langle \mathbf{A}^- \rangle_0 = 0, \tag{63}$$

in addition to Eq.(3). We leave it for future work to check whether this choice is possibly in conflict with the first gauge condition in Eq.(3). But the proffered choice would have the advantage to be manifestly invariant under color rotations and to treat the zero mode components of \mathbf{A}^- the same way in all three Gauss' equations(9). Moreover, since $\tilde{\mathbf{Q}} = \mathbf{Q}$, both charges would be strict constants of the motion, reconciling thus naive and refined considerations.

But perhaps these considerations are academic since all zero modes become sets of measure zero in the continuum limit. The solutions of the integral equation, for example, are color singlets in the strict sense. As mentioned, they are independent of the gauge choices in the zero mode sector.

8 Summary and Discussion

The approach taken here follows closely some earlier work [7]. Beginning with SU(2) pure gauge theory in (2+1) dimensions in the front form one suppresses the transverse coordinate dependence of the gluons and obtains a (1+1) dimensional gauge theory coupled to adjoint scalar matter. The present work has one major aim: We would like to get a first and rough idea on how the excitation spectrum as well as how the structure functions look in such a dimensionally reduced quantum field theory. Therefore, in order to have a tractable formalism and in contrast to earlier [7] and ongoing work [8], we suppress here by hand the dynamical impact of the topological gauge zero mode (ζ) and of the constrained zero mode (a_0). We perform furthermore a Tamm-Dancoff truncation and include only the 2-particle Fock space.

What are the results? Most important we think is the result displayed in Figure 3, namely that the solutions corresponding to color singlets ($Q = 0$) have a discrete and finite spectrum over a wide range of the harmonic resolution K . The states corresponding to color triplets ($Q = 1$) or pentuplets ($Q = 2$) can well be separated and tend to have a very large if not infinite mass. This appears to be one of the few available concrete pieces of evidences that only the color singlets can have finite mass in a non-abelian field theory. The method to identify these states is somewhat pragmatic since the model assumption on the zero mode, $a_0 = 0$, violates strict SU(2) invariance.

In Section 6 the continuum limit was established by deriving an integral equation in the manner of Bergknoff [18] for QED₁₊₁, see also [15]. As demonstrated, the continuum limit exists only for

$C = 0$, resulting for the color singlets in the integral equation

$$\omega \psi(x) = \frac{\mu^2 + 16\hat{g}^2}{x(1-x)} \psi(x) + 4\hat{g}^2 \int_0^1 \frac{dx'}{(x-x')^2} \left[4\psi(x) - \frac{(x+x')(2-x-x')}{\sqrt{x(1-x)x'(1-x')}} \psi(x') \right]. \quad (64)$$

The integral equation is identical with the one derived earlier by Bardeen *et al.* [17] and by Klebanov *et al.* [11], a remarkable fact in view that both these authors have used the light-cone gauge as opposed to the present light-cone *Coulomb* gauge.

The present model is restricted to the lowest non-trivial Fock states, those with particle number two. Fock states with three partons like $a_n^\dagger b_m^\dagger d_k^\dagger |0\rangle$ are ruled out since all matrix elements between the 2- and the 3-particle sector vanish due to color invariance. The next higher Fock-states have thus four partons: aaaa-, aabd, and bdbd-states. Based on the numerical experience with the massive and massless Schwinger model [15, 16], one can guess that the admixtures of the 4-parton states in the low lying part of the spectrum are of the order of 10^{-3} and thus probably negligible.

A rather interesting feature of the model should be mentioned. For sufficiently small variations of the mass parameter μ around the value zero the spectrum as displayed in Figure 2 can be moved up and down unchanged almost at gusto, including the case that the lowest eigenvalue coincides with zero. A trace of that survives even in the larger variations of Figure 5. It looks *as if* a mass *difference* like the one in Eq.(68) is a dimensionless number characteristic for the present model. It should be interesting to get an analytic estimate, because the mechanism allows to generate *huge mass ratios* M_2/M_1 as they are characteristic for hadronic physics.

What can one learn from this work beyond our particular play model? Let us return to the fundamental assumption $\partial_i \mathbf{A}^\mu = 0$ as in [7]. Dimensionful quantities are never strictly zero, so let us be more quantitative. In the full 3+1 dimensional treatment one would introduce an invariant mass cut-off like for example the one of Lepage and Brodsky, see [4],

$$\sum_\nu \left(\frac{m^2 + \vec{k}_\perp^2}{x(1-x)} \right)_\nu \leq \Lambda^2. \quad (65)$$

It is covariant, the sum runs over all partons ν . The scale Λ is at our disposal. For two massless gluons one obtains thus $\vec{k}_\perp^2 \leq x(1-x)\Lambda^2$. Maximizing this by $x = 1/2$ and using transverse periodic boundary conditions with $\vec{k} = \vec{n}\pi/L_\perp$ one gets $|n| \leq \Lambda L_\perp/(2\pi)$. Therefore, all transverse momenta are cut out when one *defines* the transverse length by

$$L_\perp \equiv \frac{\pi}{\Lambda}. \quad (66)$$

Only the transverse zero modes survive, and this is precisely the present model.

The fact that we have started from 2+1 dimensions weighs less. In 3+1 dimensions, the model with only transversal zero modes in the manner of [7] is only marginally more complicated due to the non-abelian commutator term. First estimates show that its impact is not dominant. With a grain of salt, the present color singlet solutions would then correspond to the helicity aligned 2^{++} -glue-balls. If one sets the cut-off scale as the typical hadronic energy $\Lambda \sim 1 \text{ GeV}$ one gets for the transversal size $L_{\perp} \sim 0.6 \text{ fm}$, a value not untypical for hadronic sizes.

One can push these simple considerations even further. The present coupling constant g is related to g_3 in 3+1 dimensions [7] by $g_3 = 2gL_{\perp}$. Our unit of mass $m_u = g/4\sqrt{\pi}$ can thus be expressed in terms of $\alpha_s = g_3^2/4\pi$ and Λ . A value of $\alpha_s \sim 0.4$ looks reasonable as compared to the empirical $\alpha_s(M_Z) \simeq 0.12$. With Eq.(66) one obtains

$$m_u = \sqrt{\alpha_s} \frac{\Lambda}{8\pi} \sim 25 \text{ MeV} , \quad (67)$$

which allows to convert our numerical results to physical units. By order of magnitude, one reads off Figure 2 for the first two states $M_1^2 \simeq 0.0018 m_0^2$ and $M_2^2 \simeq 0.038 m_0^2$, thus

$$\frac{1}{m_u^2} (M_2^2 - M_1^2) \simeq 800 , \quad M_1 \simeq 150 \text{ MeV} , \quad M_2 \simeq 600 \text{ MeV} . \quad (68)$$

These numbers are not untypical for hadrons.

In conclusion, the physical picture emerging from this work might over-stress the point but without being necessarily false: Hadrons particularly glue-balls have no transversal structure up to transversal sizes of about 0.5 fm , compare also with the recent work of van Baal [19]. The field lines are parallel due to the basic ingredient of the model, in accord with phenomenological flux-tube models. Up to these sizes, the structure resides in the longitudinal direction as mirrored in the structure functions displayed in Figure 4.

9 Acknowledgement

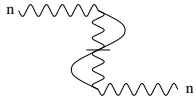
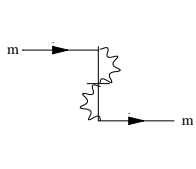
The authors thank Dr. Alex Kalloniatis for pursuing the progress of this work which would not have started without him. We have enjoyed the many discussions, but regret that we might have distracted him from his perennial fight with the constraint equation. We thank Dr. Brett van de Sande for suggesting mass renormalization and appreciate the comments of Drs. M. Burkardt and S. Dalley during their visits at the Max-Planck Institut in the summer 1995.

References

- [1] P.A.M. Dirac, *Rev.Mod.Phys.* **21** (1949) 392.
- [2] S. Weinberg, *Phys.Rev.* **150** (1966) 1313.
- [3] H.C. Pauli and S.J. Brodsky, *Phys.Rev.* **D32** (1985) 1993.
- [4] S.J. Brodsky and H.C. Pauli, ‘Light-Cone Quantization of Quantum Chromodynamics’, Lecture Notes in Physics Vol. 396, Springer-Verlag Berlin Heidelberg 1991, p. 51.
- [5] R.P. Feynman, *Phys.Rev.Lett.* **23** (1969) 1415.
- [6] S.D. Glazek, Ed., ‘The Theory of Hadrons and Light-Front QCD’, World Scientific Publishing Co, Singapore, 1995.
- [7] H.C. Pauli, A.C. Kalloniatis, and S.S. Pinsky, *Phys.Rev.* **D52** (1995) 1176.
- [8] A.C. Kalloniatis, Heidelberg preprint MPI-H-V29-1995; hep-th/9509036.
- [9] V.A. Franke, Yu.A. Novozhilov, and E.V. Prokhvatilov, *Lett.Math.Phys.* **5** (1981) 239;437.
- [10] S. Dalley and I.R. Klebanov, *Phys.Rev.* **D47** (1993) 2517.
- [11] K. Demeterfi, I.R. Klebanov, and G. Bhanot, *Nucl.Phys.* **B418** (1994) 15.
- [12] G. Bhanot, K. Demeterfi, and I.R. Klebanov, *Phys.Rev.* **D48** (1993) 4980.
- [13] F. Antonuccio and S. Dalley, Oxford preprint OUTP-9524P; hep-ph/9506456.
- [14] N.S. Manton, *Ann.Phys.(N.Y.)* **159** (1985) 220.
- [15] T. Eller, H.C. Pauli and S.J. Brodsky, *Phys.Rev.* **D35** (1987) 1493.
- [16] S. Elser, H.C. Pauli, A.C. Kalloniatis, Heidelberg preprint MPI-V17-1995; hep-th/9505069.
- [17] W.A. Bardeen, R.B. Pearson, and E. Rabinovici, *Phys.Rev.* **D21** (1980) 1039.
- [18] H. Bergknoff, *Nucl.Phys.* **B122** (1977) 215.
- [19] P. van Baal, *Nucl.Phys.* **B369** (1992) 259.

A The Matrix Elements of the Contraction Energy

Table 1: The contraction part P_C^- of the Hamiltonian is expressed in terms of Fock-space operators. The coupling constant is absorbed into the coefficient $\hat{g}^2 = \frac{g^2}{16\pi}$. As discussed in the text, one should use $C = 0$ in the calculations.

Graph	Matrix Element
 <p>A diagram showing a self-energy loop with n external legs. The loop is represented by a wavy line with a vertical line through it, and the external legs are also wavy lines.</p>	$I_n(\zeta) = \mu^2 + \hat{g}^2 \left(16 + C + 16n \sum_{k=\frac{1}{2}}^{n-\frac{1}{2}} \frac{k^2 + \zeta^2}{(k^2 - \zeta^2)^2} + \zeta^2 \sum_{m=\frac{1}{2}}^{\infty} \frac{4}{m(m^2 - \zeta^2)} \right)$
 <p>A diagram showing a vertex correction with m external legs. The vertex is represented by a wavy line with a vertical line through it, and the external legs are also wavy lines.</p>	$J_m(\zeta) = \mu^2 + \hat{g}^2 \left(16 + 8(m + \zeta) \left(\sum_{k=\frac{1}{2}}^{m-1} \frac{k^2 + \zeta^2}{(k^2 - \zeta^2)^2} + \sum_{k=1}^{m-\frac{1}{2}} \frac{1}{k^2} \right) + 4 \frac{m + \zeta}{(m - \zeta)^2} \right. \\ \left. + \zeta^2 \sum_{n=\frac{1}{2}}^{\infty} \frac{2}{n(n^2 - \zeta^2)} + \zeta(m + \zeta) \sum_{k=m+1}^{\infty} \frac{16k}{(k^2 - \zeta^2)^2} \right)$
$\frac{\pi}{L} P_C^- = \sum_{n=1}^{\infty} \frac{I_n(\zeta)}{n} a_n^\dagger a_n + \sum_{m=\frac{1}{2}}^{\infty} \frac{J_m(+\zeta)}{m + \zeta} b_m^\dagger b_m + \sum_{m=\frac{1}{2}}^{\infty} \frac{J_m(-\zeta)}{m - \zeta} d_m^\dagger d_m$	

B The Matrix Elements of the Seagull Energy

Table 2: The seagull part P_S^- of the Hamiltonian is expressed in terms of Fock-space operators. The coupling constant is absorbed into the coefficient $\hat{g}^2 = \frac{g^2}{16\pi}$. The indices of a and a^\dagger are integers, those of b, b^\dagger, d and d^\dagger half-integers. The Kronecker delta $\delta_{n_3+n_4}^{n_1+n_2}$ referring to momentum conservation in $S(n_1, n_2; n_3, n_4)$ is not kept track of explicitly.

Graph	Matrix Element
	$S_{bb}(n_1, n_2; n_3, n_4; \zeta) = \left(\sqrt{\frac{n_1+\zeta}{n_3+\zeta}} + \sqrt{\frac{n_3+\zeta}{n_1+\zeta}} \right) \left(\sqrt{\frac{n_2+\zeta}{n_4+\zeta}} + \sqrt{\frac{n_4+\zeta}{n_2+\zeta}} \right) \frac{\hat{g}^2}{(n_1-n_3)^2}$
	$S_{bd}(n_1, n_2; n_3, n_4; \zeta) = \left(\sqrt{\frac{n_1+\zeta}{n_3+\zeta}} + \sqrt{\frac{n_3+\zeta}{n_1+\zeta}} \right) \left(\sqrt{\frac{n_2-\zeta}{n_4-\zeta}} + \sqrt{\frac{n_4-\zeta}{n_2-\zeta}} \right) \frac{(-2)\hat{g}^2}{(n_1-n_3)^2}$ $+ \left(\sqrt{\frac{n_2-\zeta}{n_1+\zeta}} - \sqrt{\frac{n_1+\zeta}{n_2-\zeta}} \right) \left(\sqrt{\frac{n_4-\zeta}{n_3+\zeta}} - \sqrt{\frac{n_3+\zeta}{n_4-\zeta}} \right) \frac{2\hat{g}^2}{(n_1+n_2)^2}$
	$S_{ab}(n_1, n_2; n_3, n_4; \zeta) = \left(\sqrt{\frac{n_4}{n_2+\zeta}} + \sqrt{\frac{n_2+\zeta}{n_4}} \right) \left(\sqrt{\frac{n_1}{n_3+\zeta}} + \sqrt{\frac{n_3+\zeta}{n_1}} \right) \frac{2\hat{g}^2}{(n_1-n_3-\zeta)^2}$ $+ \left(\sqrt{\frac{n_1}{n_2+\zeta}} - \sqrt{\frac{n_2+\zeta}{n_1}} \right) \left(\sqrt{\frac{n_4}{n_3+\zeta}} - \sqrt{\frac{n_3+\zeta}{n_4}} \right) \frac{2\hat{g}^2}{(n_1+n_2+\zeta)^2}$
	$S_{aa}(n_1, n_2; n_3, n_4; \zeta) = \left(\sqrt{\frac{n_1}{n_3+\zeta}} + \sqrt{\frac{n_3+\zeta}{n_1}} \right) \left(\sqrt{\frac{n_2}{n_4-\zeta}} + \sqrt{\frac{n_4-\zeta}{n_2}} \right) \frac{(-2\hat{g}^2)}{(n_1-n_3+\zeta)^2}$
$\frac{\pi}{L} P_S^- = \sum_{n_i} S_{bb}(n_1, n_2; n_3, n_4; \zeta) b_{n_1}^\dagger b_{n_2}^\dagger b_{n_3} b_{n_4} + S_{bb}(n_1, n_2; n_3, n_4; -\zeta) d_{n_1}^\dagger d_{n_2}^\dagger d_{n_3} d_{n_4}$ $+ \sum_{n_i} S_{bd}(n_1, n_2; n_3, n_4; \zeta) b_{n_1}^\dagger d_{n_2}^\dagger b_{n_3} d_{n_4} +$ $+ \sum_{n_i} S_{aa}(n_1, n_2; n_3, n_4; \zeta) (a_{n_1}^\dagger a_{n_2}^\dagger b_{n_3} d_{n_4} + d_{n_4}^\dagger b_{n_3}^\dagger a_{n_2} a_{n_1})$ $+ \sum_{n_i} S_{ab}(n_1, n_2; n_3, n_4; \zeta) a_{n_1}^\dagger b_{n_2}^\dagger b_{n_3} a_{n_4} + S_{ab}(n_1, n_2; n_3, n_4; -\zeta) a_{n_1}^\dagger d_{n_2}^\dagger d_{n_3} a_{n_4}$	

C The Matrix Elements of the Fork Energy

Table 3: The fork part P_F^- of the Hamiltonian is expressed in terms of Fock-space operators. The coupling constant is absorbed into the coefficient $\hat{g}^2 = \frac{g^2}{16\pi}$. The indices of a and a^\dagger are integers, those of b, b^\dagger, d and d^\dagger half-integers. The Kronecker delta $\delta_{n_2+n_3+n_4}^{n_1}$ referring to momentum conservation in $F(n_1; n_2, n_3, n_4)$ is not kept track of explicitly.

Graph	Matrix Element
	$F_{ba}(n_1; n_2, n_3, n_4; \zeta) = \left(\sqrt{\frac{n_1+\zeta}{n_2+\zeta}} + \sqrt{\frac{n_2+\zeta}{n_1+\zeta}} \right) \left(\sqrt{\frac{n_3+\zeta}{n_4-\zeta}} - \sqrt{\frac{n_4-\zeta}{n_3+\zeta}} \right) \frac{2\hat{g}^2}{(n_1-n_2)^2}$
	$F_{bb}(n_1; n_2, n_3, n_4; \zeta) = \left(\sqrt{\frac{n_1+\zeta}{n_2}} + \sqrt{\frac{n_2}{n_1+\zeta}} \right) \left(\sqrt{\frac{n_4+\zeta}{n_3}} - \sqrt{\frac{n_3}{n_4+\zeta}} \right) \frac{2\hat{g}^2}{(n_1-n_2+\zeta)^2}$
	$F_{ab}(n_1; n_2, n_3, n_4; \zeta) = \left(\sqrt{\frac{n_2+\zeta}{n_1}} + \sqrt{\frac{n_1}{n_2+\zeta}} \right) \left(\sqrt{\frac{n_4}{n_3-\zeta}} - \sqrt{\frac{n_3-\zeta}{n_4}} \right) \frac{2\hat{g}^2}{(n_1-n_2-\zeta)^2}$
	$+ \left(\sqrt{\frac{n_3-\zeta}{n_1}} + \sqrt{\frac{n_1}{n_3-\zeta}} \right) \left(\sqrt{\frac{n_4}{n_2+\zeta}} - \sqrt{\frac{n_2+\zeta}{n_4}} \right) \frac{2\hat{g}^2}{(n_1-n_3+\zeta)^2}$
$\begin{aligned} \frac{\pi}{L} P_F^- &= \sum_{n_i} F_{ba}(n_1; n_2, n_3, n_4; \zeta) b_{n_1}^\dagger b_{n_2} b_{n_3} d_{n_4} + F_{ba}(n_1; n_2, n_3, n_4; -\zeta) d_{n_1}^\dagger d_{n_2} d_{n_3} b_{n_4} \\ &+ \sum_{n_i} F_{bb}(n_1; n_2, n_3, n_4; \zeta) b_{n_1}^\dagger a_{n_2} a_{n_3} b_{n_4} + F_{bb}(n_1; n_2, n_3, n_4; -\zeta) d_{n_1}^\dagger a_{n_2} a_{n_3} d_{n_4} \\ &+ \sum_{n_i} F_{ab}(n_1; n_2, n_3, n_4; \zeta) a_{n_1}^\dagger b_{n_2} d_{n_3} a_{n_4} \quad + h.c. \end{aligned}$	